Collective Coherent Control: Synchronization of Polarization in Ferroelectric $PbTiO_3$ by Shaped THz Fields

Tingting Qi,[1] Young-Han Shin,[1] Ka-Lo Yeh,[2] Keith A. Nelson,[2] and Andrew M. Rappe[1]

[1]*The Makineni Theoretical Laboratories, Department of Chemistry, University of Pennsylvania, Philadelphia, Pennsylvania 19104–6323, USA*

[2]*Department of Chemistry, Massachusetts Institute of Technology, Cambridge, Massachusetts 02139, USA*

(Received 16 November 2008; published 19 June 2009)

We show that properly shaped terahertz (THz) fields can be used to move ions in ferroelectric crystals from their positions in an initial domain orientation along well-defined collective microscopic paths into the positions they occupy in a new domain orientation. Collective coherent control will enable direct observation of fast highly nonlinear material responses and far-from-equilibrium structures that can be harnessed in electro-optic devices and nonvolatile computer memory.

DOI: 10.1103/PhysRevLett.102.247603 PACS numbers: 77.80.Fm, 71.15.Pd, 77.84.Dy, 87.50.U−

Coherent optical control over ultrafast molecular behavior including chemical reactions has been explored in recent years [1], spurred by the application of optimal control theory and related methods [2,3] and by the development of femtosecond pulse shaping techniques [4–6] through which complex optical waveforms have been crafted and optimized to induce specified molecular responses. Here, we propose and model theoretically the extension of coherent control to collective structural change. We show through numerical simulations that temporally shaped THz fields can be used to induce ferroelectric domain switching with extensive control over the collective microscopic pathway from initial to final structure, in a coherent process that is very different from the conventional stepwise switching mechanism [7].

Perovskite ferroelectric crystals have simple collective lattice vibrational modes that describe the microscopic pathways along which structural change occurs [see Fig. 1(a)]. For this reason, these crystals are prototypes for the study of collective structural rearrangements, with many modelling studies interrogating both static and dynamic aspects of their phase transitions [8,9]. A particularly important aspect is domain switching, the process of reorienting part or all of a domain so that its macroscopic polarization points in a different direction. We and others [10–14] have sought to illuminate how microscopic interatomic interactions affect the rate and mechanism of ferroelectric domain switching.

In the tetragonal phase of lead titanate ($PbTiO_3$, PTO), the crystal has two domain orientations characterized by opposite polarization directions along the tetragonal axis with symmetrically equivalent ground states separated by an energy barrier. The polarization direction can be reversed under an electric field. This is exploited extensively in ferroelectric memory devices, so the dynamics of domain switching have been of technological as well as fundamental interest. There is great experimental interest in rapid ferroelectric polarization switching under strong electric fields, with most experimental approaches limited to the thin film regime [7,15–17]. Most studies of polarization reversal focus on domain wall properties and dynamics under the influence of an electric field that is applied through electrodes at the sample surfaces [13,18,19]. Earlier attempts to control crystalline soft modes and phase transitions through impulsive stimulated Raman scattering used nonresonant optical pulses without tailored pulse profiles [20–22] and were based on simple models for the impulsively driven lattice vibrations and the crystalline responses to them; so far, such attempts have failed to find experimental validation because the high light intensities needed to reach sufficient vibrational amplitudes far exceed typical material damage thresholds.

In contrast, here we explore the fundamental limit of the polarization switching time of ferroelectric PTO under the

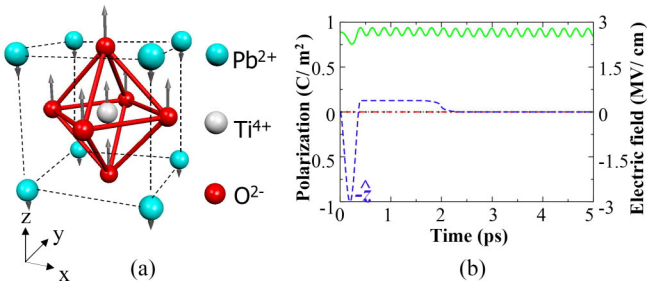

FIG. 1 (color online). (a) PTO unit cell in the tetragonal ferroelectric phase, with a $+\hat{z}$ domain orientation. The soft vibrational mode is indicated by the arrows on the ions. (b) Time-dependent lattice response to a single asymmetric THz pulse (shown by a blue dashed line) with its large lobe polarized along the $-\hat{z}$ direction, i.e., ''antiparallel'' to the static ferroelectric polarization. The z-component P_z (shown by a green solid line) oscillates about its static nonzero value as the Ti and other ions oscillate about their lattice positions in the $+z$ domain. No significant responses of the other components P_x and P_y (shown by a black dotted and a red dashed-dotted line, respectively) about their static values of zero are induced.

coherent control of a THz-frequency electromagnetic driving field that permeates the sample and is resonant with its soft mode frequency. Using a well validated atomic potential model of PTO [13,23], we consider the coherent reorientation of a large region, without domain wall formation or movement, and we consider a THz-frequency driving field with tailored amplitude, phase, and polarization profiles, motivated by recent progress in the generation of large-amplitude shaped THz fields and in the observation of anharmonic responses of ferroelectric soft modes to them [24]. We examine the possibility of coherent control over domain reversal to ''read'' or ''write'' bulk ferroelectric data storage media on picosecond time scales.

We carried out molecular dynamics (MD) simulations of PTO with a $6 \times 6 \times 6$ supercell using a classical potential formulated and parameterized [23] to reproduce the energies and all atomic forces encountered in Car-Parrinello simulations for a large set of thermally accessed structures. The interatomic potential consists of four parts: a term with the bond-valence [25] potential energy form (but modified numerical constants), a Coulomb potential energy term with modified charges, a r^{-12} repulsion term, and a harmonic term to reduce the angle tilts of octahedral cages. This potential [23] reproduces the ferroelectric behavior of PTO accurately without being fit to any experimental observations [9,13,26].

To simulate THz experiments, we set the tetragonal lattice constants to the experimental values ($a = 3.9$ Å, $c = 4.15$ Å) and one or more electric field pulses were applied to the system. All the pulses had an asymmetric electric field profile with a large-amplitude lobe of about 150 fs duration (to include frequency components up to about 6.6 THz) and a lower-amplitude lobe of longer duration in the opposite polarity. The electric field integrates to zero as required for optical pulses [Fig. 1(b)]. The asymmetric field profile is well suited for driving nonlinear responses in the direction of the large-amplitude lobe. Even shorter pulses could also drive polarization oscillations similar to the pulses we chose. However, to flip polarization with the same number of shorter pulses, much higher electric field amplitude is required, which is very challenging to generate and could lead to material damage.

To switch the polarization from $+\hat{z}$ to $-\hat{z}$, the most direct way is to apply electric field pulses along $-\hat{z}$. Figure 1(b) shows that applying a $-\hat{z}$-oriented electric field pulse causes the z-component of the polarization (P_z) to oscillate in time about its nonzero static value. The other polarization components (P_x and P_y) remain essentially zero. The oscillation period of about 240 fs, which corresponds to 4.2 THz, is independent of pulse magnitude, indicating an essentially harmonic mode (the Pb-O or so-called Last mode) at these amplitudes. The phonon frequency is in good agreement with density-functional theory (DFT) calculations and the experimental value [27] of 4.5 THz.

In order to reorient the lattice polarization, the coherent vibrational amplitude must be made large enough to overcome the potential energy barrier between the two stable polarization states. The P_z vibrational coherence could be reduced or enhanced by successive pulses depending on their timing. As shown in Fig. 2(a), polarization reversal can be achieved within 15 ps with seven pulses of amplitude 3 MV/cm. In order to suppress coherent return of the polarization to its original direction and multiple successive domain flipping events, we applied one additional $-\hat{z}$-oriented pulse out of phase with the P_z oscillations. This guaranteed that after the system acquires sufficient energy to cross the barrier freely, we can then trap it in the desired polarization state. It is important to note that the out-of-phase pulse cools down the system substantially ($\approx$95 K) since much of the energy is in the coherent mode after the first six pulses. In order to avoid excessive heating of the system, such an out-of-phase pulse could be useful not only at 0 K but also at finite temperature.

It is well known from the quasi-dc limit that polarization rotation offers lower-energy pathways to polarization flip-

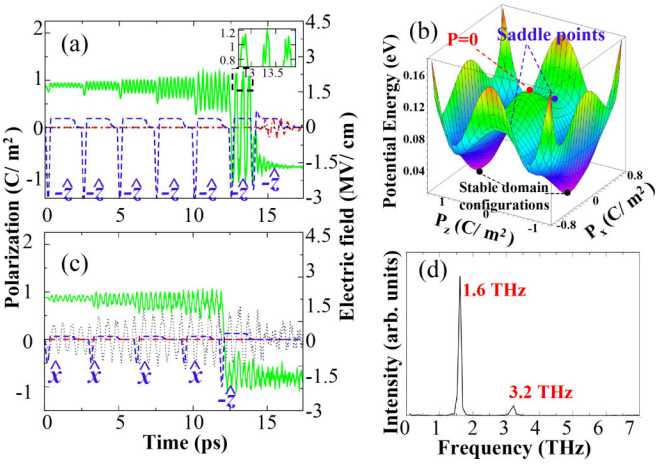

FIG. 2 (color online). Collective coherent control over ferroelectric polarization with shaped THz waveforms. (a) Sequence of seven asymmetric THz pulses (blue dashed line), all z-polarized with large lobes (3 MV/cm) along the $-\hat{z}$ direction. Each successive pulse increases the polarization (P_z is shown by a green solid line) oscillation amplitude by driving the soft mode in phase with the oscillation already present. The time interval between pulses is an integer number of soft mode periods which gradually grow longer due to anharmonicity. (b) Lattice potential energy surface (PES) with respect to P_x and P_z, calculated using our MD model. A PES local maximum appears at the high-symmetry cubic structure with $P_x = P_z = 0$. The z-polarized THz field in (a) drives the system over this potential energy barrier. Domain switching can occur with lower energies along trajectories that pass through or near the saddle points in the PES. (c) Sequence of four THz pulses with $\hat{x}$-oriented fields followed by a final THz pulse with $-\hat{z}$-oriented field. (d) Power spectrum from Fourier transformation of P_x and P_z in (c). A strong peak stems from P_x oscillations at the 1.6 THz phonon frequency. The smaller peak shows the second harmonic frequency of oscillations in P_z.

ping than directly surmounting the local potential energy maximum at the high-symmetry cubic lattice configuration. Atomistically, polarization rotation corresponds to a trajectory for Ti that goes around, rather than through, the unit cell center [28]. We therefore investigated coherently controlled trajectories involving significant ionic motions and lattice polarization components along the $\hat{x}$ and/or $\hat{y}$ directions as well as $\hat{z}$, exploring much more of the three-dimensional lattice potential energy surface (PES). Figure 2(b) shows the lattice potential energy obtained from our MD model as a function of P_z and P_x. The energies required to reach the high-symmetry PES local maximum and a saddle point (ΔE_z and ΔE_x, respectively) are compared in Table I. The saddle point energy is about 20% lower, offering lower-energy switching trajectories than those that pass through the PES maximum.

We conducted MD simulations with sequences of $\hat{x}$- and $\hat{z}$-polarized asymmetric THz pulses rather than all $\hat{z}$-polarized pulses as described earlier. Figure 2(c) shows an example with four $\hat{x}$-polarized pulses (with large lobes of amplitude 1 MV/cm along $+\hat{x}$) followed by one $\hat{z}$-polarized pulse (with a large lobe of amplitude 2 MV/cm along $-\hat{z}$). After a single $\hat{x}$-oriented pulse, the simulation shows that both P_x and P_z oscillations were excited, corresponding to polarization rotation in the $\hat{x}\,\hat{z}$ plane. The power spectrum in Fig. 2(d) shows that the frequency for P_z oscillation was twice that of P_x (1.6 THz), which is a consequence of the lattice symmetry about the $x = 0$ plane. The curvature of the PES draws the z-component of the polarization toward smaller values when the x-component undergoes an excursion toward positive or (symmetry-equivalent) negative values. For example, the Ti ion moves toward the $z = 0$ plane when it is displaced in either direction from the $x = 0$ plane. Thus, each half-cycle of P_x corresponds to a full cycle of P_z. The oscillation amplitude of P_z depends quadratically on that of P_x until highly anharmonic regimes are reached, and the P_z response would give rise to z-polarized frequency-doubling of x-polarized incident THz radiation.

The simulation results in Fig. 2(c) show that each successive x-polarized pulse increases the lattice polarization rotation amplitude, as each time P_x reaches a maximum excursion away from zero, P_z reaches a maximum excursion away from its initial nonzero value toward a smaller value. After the fourth $\hat{x}$-oriented pulse, P_x exceeds P_z at the extrema of oscillation, which means that the polarization is rotating more than 45° and approaching the saddle point of the PES. Finally, a $-\hat{z}$-oriented pulse is applied to push the system over the saddle point. This approach [Fig. 2(c)] switches the ferroelectric domain more efficiently than the former method [Fig. 2(a)], in terms of the number of pulses, their peak magnitudes, and their integrated energy. The result illustrates the value of shaping the polarization as well as the amplitude and phase profiles of the THz control field. Polarization shaping has proved valuable in some examples of molecular coherent control with visible light fields [24].

TABLE I. Comparison of potential energy local maximum ΔE_z vs saddle point ΔE_x for polarization switching in PTO.

	DFT	Our MD model
ΔE_z (eV/unit cell)	0.168	0.143
ΔE_x (eV/unit cell)	0.136	0.110
$\Delta E_x/\Delta E_z$	0.81	0.77

Maintaining coherence at finite temperature is more challenging than at 0 K because the increase in random fluctuations makes the final state more difficult to predict. The increased temperature changes several key factors that affect the switching process. First, coherence is lost more rapidly due to faster energy dissipation and pure dephasing. Second, the ferroelectric well depth decreases with higher temperature, as the higher entropy of the paraelectric state makes its free energy more competitive with that of the ferroelectric state. These two effects compete, with the first inhibiting coherence and the second facilitating domain flipping.

To guide our understanding of finite temperature domain switching, we concentrate on the response of the domain to a single $-\hat{z}$-oriented pulse. For a single pulse to reorient the polarization, the pulse strength should be sufficient for the system to visit the potential energy minimum of the opposite polarization, yet not strong enough for the polarization to flip back. Our findings are summarized in Fig. 3. Because of thermal fluctuations, the same initial conditions can yield different results, with flipping success being a probabilistic event. We chose four different initial sample temperatures (50, 100, 200, and 300 K are shown by a black solid, a red dotted, a green dashed, and a blue dashed-dotted line, respectively) to analyze statistically. For each temperature, we traced 250 trajectories starting

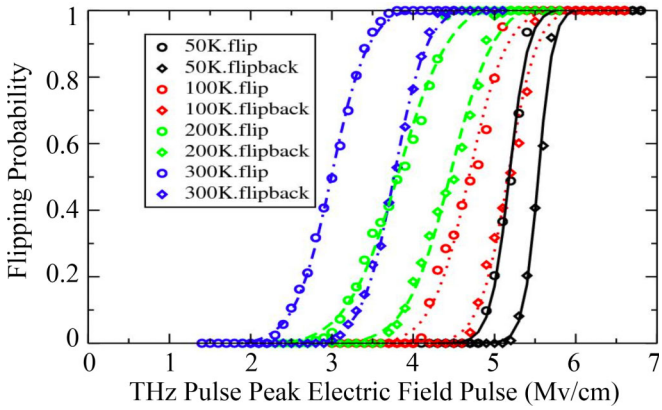

FIG. 3 (color online). The probability of at least a single "flip" or at least two flips (denoted "flipback") of polarization in response to a single $-\hat{z}$-oriented pulse with varied peak field amplitudes at different temperatures. At higher temperatures, lower field amplitudes are sufficient to flip the domain, while stronger dissipation in the new domain suppresses flipback for a wider range of field amplitudes.

TABLE II. Fitting parameters of flipping probabilities at different finite temperatures according to Eq. (1). Temperature is in Kelvin, α is unitless, and field E_0 is in MV/cm.

Temp.	$\alpha(T,1)$	$\alpha(T,2)$	$E_0(T,1)$	$E_0(T,2)$	$E_0(T,2)-E_0(T,1)$
50	22.43	30.75	5.18	5.54	0.36
100	11.25	16.03	4.68	5.16	0.48
200	8.32	11.39	3.78	4.43	0.65
300	6.64	9.51	2.99	3.76	0.77

from different equilibrated states irradiated by a single $-\hat{z}$-oriented pulse. To avoid excessive heating of the material, we limited the amplitude of the short duration electric field lobe. In Fig. 3, the circles indicate the probability that the system climbs over the PES barrier before damping reduces the energy in the coherent mode to below the barrier height (flip), and diamonds indicate the probability that it crosses back to the original domain orientation (flipback). Hence, the difference between these two datasets is the probability of exactly one flip reversing a domain. Equation (1) fits the simulation results well (the fitting parameters are presented in Table II):

$$\mathcal{P}(E,T,n)=\frac{1}{2}+\frac{1}{2}\tanh\left(\alpha\left[\frac{E}{E_0}-1\right]\right) \qquad (1)$$

where α and E_0 depend on temperature (T) and n. The E_0 values for both "flip" ($n=1$) and "flipback" ($n=2$) decrease monotonically with T. $E_0(T,1)$ closely tracks the T-dependent free energy barrier, while $E_0(T,2)$ is higher than $E_0(T,1)$ because of damping within one half period. This effect nearly doubles the range of field amplitudes over which single flipping is achieved as T is raised from 50 to 300 K. The trends from MD simulations illustrate well the competing effects introduced by temperature. We find that the required minimum magnitude of the pulse decreases as the temperature increases because of the decreasing ferroelectric double well depth. Meanwhile, the range of pulse magnitudes that achieve "flip" without "flipback" is larger at higher temperatures because of increased dissipation.

Through MD simulations, we have demonstrated that collective coherent control over ferroelectric domain orientation should be possible through the use of shaped THz pulse sequences. Shaping of all aspects of the THz fields—the amplitude, phase, and polarization profiles—can contribute substantially to coherent control over collective material dynamics and structure.

T. Q. was supported by the Office of Naval Research Grant No. N00014-09-1-0157 and A. M. R. by the Department of Energy, Office of Basic Energy Sciences Grant No. DE-FG02-07ER46431. Computational support was provided by a Challenge grant from High-Performance Computing. K. A. N and K.-L. Y. were supported by the Office of Naval Research Grant No. N00014-06-1-0459, and by the National Science Foundation Grant No. CHE06-16939. Y.-H. S. was supported by the Brain Korea 21 Project 2009.

[1] P. Nuernberger, G. Vogt, T. Brixner, and G. Gerber, Phys. Chem. Chem. Phys. **9**, 2470 (2007).
[2] S. Shi and H. Rabitz, Chem. Phys. **139**, 185 (1989).
[3] R. J. Levis and H. A. Rabitz, J. Phys. Chem. A **106**, 6427 (2002).
[4] M. M. Wefers and K. A. Nelson, Opt. Lett. **20**, 1047 (1995).
[5] A. M. Weiner, Rev. Sci. Instrum. **71**, 1929 (2000).
[6] T. Brixner and G. Gerber, Opt. Lett. **26**, 557 (2001).
[7] T. Tybell, P. Paruch, T. Giamarchi, and J.-M. Triscone, Phys. Rev. Lett. **89**, 097601 (2002).
[8] S. R. Phillpot and V. Gopalan, Appl. Phys. Lett. **84**, 1916 (2004).
[9] Y.-H. Shin, J.-Y. Son, B.-J. Lee, I. Grinberg, and A. M. Rappe, Condens. Matter Phys. **20**, 015224 (2008).
[10] D. Damjanovic, Rep. Prog. Phys. **61**, 1267 (1998).
[11] J. Y. Li, R. C. Rogan, E. Ustundag, and K. Bhattacharya, Nature Mater. **4**, 776 (2005).
[12] J. Padilla, W. Zhong, and D. Vanderbilt, Phys. Rev. B **53**, R5969 (1996).
[13] Y.-H. Shin, I. Grinberg, I.-W. Chen, and A. M. Rappe, Nature (London) **449**, 881 (2007).
[14] A. M. Bratkovsky and A. P. Levanyuk, Phys. Rev. Lett. **84**, 3177 (2000).
[15] A. Grigoriev, D. H. Do, D. M. Kim, C. B. Eom, B. Adams, E. M. Dufresne, and P. G. Evans, Phys. Rev. Lett. **96**, 187601 (2006).
[16] L. M. Eng, Nanotechnology **10**, 405 (1999).
[17] M. P. McCormick and J. C. Larsen, Geophys. Res. Lett. **15**, 907 (1988).
[18] S. V. Kalinin, C. Y. Johnson, and D. A. Bonnell, J. Appl. Phys. **91**, 3816 (2002).
[19] T. Tybell, C. H. Ahn, and J.-M. Triscone, Appl. Phys. Lett. **75**, 856 (1999).
[20] Y. X. Yan, E. B. Gamble, and K. A. Nelson, J. Chem. Phys. **83**, 5391 (1985).
[21] S. Fahy and R. Merlin, Phys. Rev. Lett. **73**, 1122 (1994).
[22] K. A. Nelson, *Coherent Control: Optics, Molecules, and Materials* (Springer-Verlag, Berlin, 1995).
[23] Y.-H. Shin, V. R. Cooper, I. Grinberg, and A. M. Rappe, Phys. Rev. B **71**, 054104 (2005).
[24] J. Hebling, K.-L. Yeh, M. C. Hoffmann, and K. A. Nelson, IEEE J. Sel. Top. Quantum Electron. **14**, 345 (2008).
[25] I. D. Brown, in *Structure and Bonding in Crystals II*, edited by M. O'Keeffe and A. Navrotsky (Academic Press, New York, 1981), pp. 1–30.
[26] P. Juhas, I. Grinberg, A. M. Rappe, W. Dmowski, T. Egami, and P. K. Davies, Phys. Rev. B **69**, 214101 (2004).
[27] C. M. Foster, Z. Li, M. Grimsditch, S.-K. Chan, and D. J. Lam, Phys. Rev. B **48**, 10160 (1993).
[28] S. Fukao, J. P. McClure, A. Ito, T. Sato, I. Kimura, T. Tsuda, and S. Kato, Geophys. Res. Lett. **15**, 768 (1988).